The Astrophysical Journal Letters, 935:L22 (6pp), 2022 August 20 https://doi.org/10.3847/2041-8213/ac874f

Typhon: A Polar Stream from the Outer Halo Raining through the Solar Neighborhood

Wassim Tenachi[1], Pierre-Antoine Oria[1], Rodrigo Ibata[1], Benoit Famaey[1], Zhen Yuan[1], Anke Arentsen[1], Nicolas Martin[1], and Akshara Viswanathan[2]
[1] Université de Strasbourg, CNRS, Observatoire astronomique de Strasbourg, UMR 7550, F-67000 Strasbourg, France; wassim.tenachi@astro.unistra.fr
[2] Kapteyn Astronomical Institute, University of Groningen, Postbus 800, 9700 AV, Groningen, the Netherlands
Received 2022 June 21; revised 2022 August 2; accepted 2022 August 2; published 2022 August 17

Abstract

We report on the discovery in the Gaia DR3 astrometric and spectroscopic catalog of a new polar stream that is found as an overdensity in action space. This structure is unique as it has an extremely large apocenter distance, reaching beyond 100 kpc, and yet is detected as a coherent moving structure in the solar neighborhood with a width of ∼4 kpc. A subsample of these stars that was fortuitously observed by LAMOST has a mean spectroscopic metallicity of $\langle [Fe/H] \rangle = -1.60^{+0.15}_{-0.16}$ dex and possesses a resolved metallicity dispersion of $\sigma([Fe/H]) = 0.32^{+0.17}_{-0.06}$ dex. The physical width of the stream, the metallicity dispersion, and the vertical action spread indicate that the progenitor was a dwarf galaxy. The existence of such a coherent and highly radial structure at their pericenters in the vicinity of the Sun suggests that many other dwarf galaxy fragments may be lurking in the outer halo.

Unified Astronomy Thesaurus concepts: Galaxies (573); Stellar streams (2166); Milky Way dynamics (1051); Local Group (929); Milky Way stellar halo (1060)

Supporting material: machine-readable table

1. Introduction

One of the principal goals of the Gaia space mission (Gaia Collaboration et al. 2016) is to survey the Milky Way, so as to allow us to understand how our home galaxy was built up over cosmic time. Although we only observe the end state of this majestic structure, fortunately the processes of formation and growth have left copious amounts of evidence in the form of debris that is now scattered throughout our galaxy (Belokurov et al. 2006; Shipp et al. 2018; Ibata et al. 2021b; Malhan et al. 2022). Some of these residues are due to the accretion of small galaxies and globular clusters, which disrupted under the action of tidal forces, leaving long stellar streams. In some cases they can still remain as elongated structures, many billion years after the dissolution of their progenitors (Helmi 2008). Studying these structures is of great importance since their trajectories probe the galactic acceleration field and the underlying dark matter distribution (e.g., Koposov et al. 2010; Sanders & Binney 2013; Malhan & Ibata 2019; Ibata et al. 2021a).

A particularly powerful means to uncover such fossil remnants is by searching for groups of stars with common integrals of motion. Action coordinates are perhaps the best choice for this, as they are adiabatic invariants that will have been preserved along orbits if the Milky Way's potential evolved only slowly through time (Binney & Tremaine 2011). However, to transform our stellar measurements into actions (and their conjugate angles), we require the full six-dimensional positions and velocities. With present instrumentation this is only achievable close to the solar position in the galaxy.

The Gaia mission has recently made accessible its third data release (DR3; Gaia Collaboration 2022) of its all-sky survey. It contains approximately 33 million stars with mean radial velocities down to $G \sim 15$, which, complemented with the excellent proper motions and parallaxes published in the earlier EDR3 release (Gaia Collaboration et al. 2021), provide the required phase-space constraints. Because the DR3 radial velocity limit is quite shallow, it almost exclusively probes the very nearby regions of the galaxy (the median distance of the sample with 10σ parallaxes is only 1.26 kpc). In the vicinity of the Sun, dynamical times are short and tidal debris are expected to phase-mix rapidly (Helmi et al. 1999, 2003), erasing any initial stream-like coherence that might have been present.

In this contribution we show that, surprisingly and contrary to those expectations, the solar neighborhood contains a very wide yet kinematically coherent metal-poor stellar stream, which we name Typhon,[3] whose apocenter reaches out to >100 kpc—the edge of the Galactic halo.

2. Selection

From the Gaia DR3 catalog, we select the 25,355,580 stars with well-constrained distances ($\varpi/\delta\varpi > 10$), radial velocities measured by Gaia's Radial Velocity Spectrometer (RVS) instrument (Recio-Blanco et al. 2022), having at least a five-parameter astrometric solution, and with magnitudes in the ranges $0 \leqslant G \leqslant 22$, $0 \leqslant G_{BP} \leqslant 30$, and $0 \leqslant G_{RP} \leqslant 30$. To convert the apparent motions to motions in a frame[4] at rest with respect to the galaxy, we assume that the Sun is located at $(x, y, z)_\odot = (-8.2240, 0, 0.0028)$ kpc (solar radius from Bovy 2020 and z-position of the Sun from Widmark et al. 2021), and that it moves with a peculiar velocity $(v_x, v_y, v_z)_\odot = (11.10, 7.20, 7.25)$ km s^{-1} (Schonrich et al. 2010, with the ϕ-direction velocity from Bovy 2020), and we take the circular velocity at the solar radius to be 243 km s^{-1} (Bovy 2020). We use the resulting phase-space measurements to derive the orbital parameters of the stars, including the

[3] The serpent Typhon is the child of Gaia and Tartarus (the deep abyss) in Greek myth.
[4] Throughout the Letter, we use a right-handed Galactic Cartesian coordinate system.

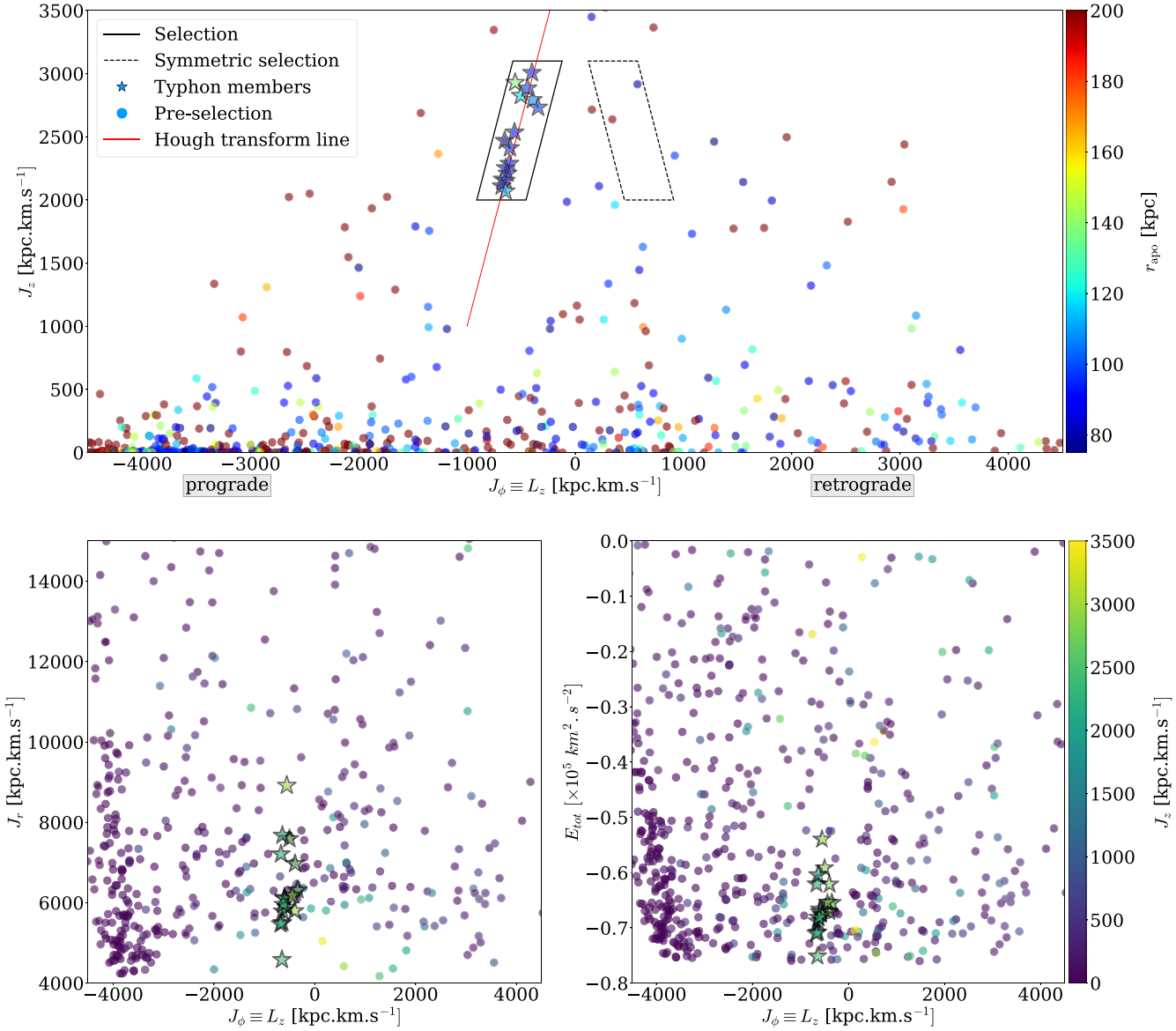

Figure 1. Actions and total energy of Typhon members (indicated by star symbols) and of the 573 preselected stars having $\varpi/\delta\varpi > 10$, $r_{\rm apo} > 75$ kpc, and $d_\odot < 4$ kpc (denoted by circles). Stars are colored by their apocenter values in the top panel and and by their vertical action values in the bottom row of panels. Top panel: (J_ϕ, J_z) plane used for the selection where the overdensity was discovered. The most significant detection obtained using a Hough transform technique (Illingworth & Kittler 1988) on stars with $J_z > 1000$ kpc km s^{-1} (i.e., with large departures from the Galactic midplane) is shown with a red line. This line runs through the Typhon structure. The parallelogram selection of the structure is depicted in a solid line encompassing 16 stars, and is defined by $J_z \in [2000, 3100]$ kpc km s^{-1} and $3.3J_\phi + 3500$ kpc km s^{-1} $< J_z < 3.3J_\phi + 5000$ kpc km s^{-1}. The symmetric (retrograde) selection with respect to the $J_\phi = 0$ line is shown with a dashed line. Bottom left and bottom right panels show the (J_ϕ, J_r) and (J_ϕ, $E_{\rm tot}$) planes, respectively.

pericenter and apocenter distances, as well as action-angle coordinates calculated using the AGAMA package (Vasiliev 2019) in a realistic potential model (McMillan 2017) for the Milky Way. Since we are particularly interested in finding debris from the outer halo that could be associated to ancient merger events, we impose an apocenter cut at $r_{\rm apo} > 75$ kpc, which yields a subsample of 870 stars

Further analysis is performed in the space of actions (J_r, J_ϕ, J_z), which encode, respectively, the amplitude of orbital motion in the radial, azimuthal, and vertical directions. In particular, we plot the (J_ϕ, J_z) projection colored by r_{apo} in Figure 1. There, a polar structure can be spotted as a tight, almost vertical, linear grouping between ($J_\phi \sim -650$ kpc km s^{-1}, $J_z \sim 2100$ kpc km s^{-1}) and ($J_\phi \sim -400$ kpc km s^{-1}, $J_z \sim 3000$ kpc km s^{-1}). We find that this feature is most striking when the sample is limited to stars with heliocentric distances $d_\odot < 4$ kpc, approximately at the limit of useful 6D phase-space data in the DR3 catalog. In particular, performing the Hough transformation (Illingworth & Kittler 1988) line detection technique on the stars in the (J_ϕ, J_z) plane (binning the action data into pixels of size 30 kpc km s^{-1} on a side and adopting a 1° discretization for the angle of the fitted lines), we find that the most significant linear grouping of stars with $J_z > 1000$ kpc km s^{-1} (i.e., that experience large excursions from the Galactic midplane) corresponds to this quasi-linear overdensity (red line in Figure 1). These 16 stars possess similar apocenter distances ($r_{\rm apo} \approx 100$ kpc), and are also highly correlated in the angle coordinates (θ_r, θ_ϕ, θ_z) conjugate to the actions.

We then separate this structure from the bulk of the data by applying a simple parallelogram selection in the (J_ϕ, J_z) plane,

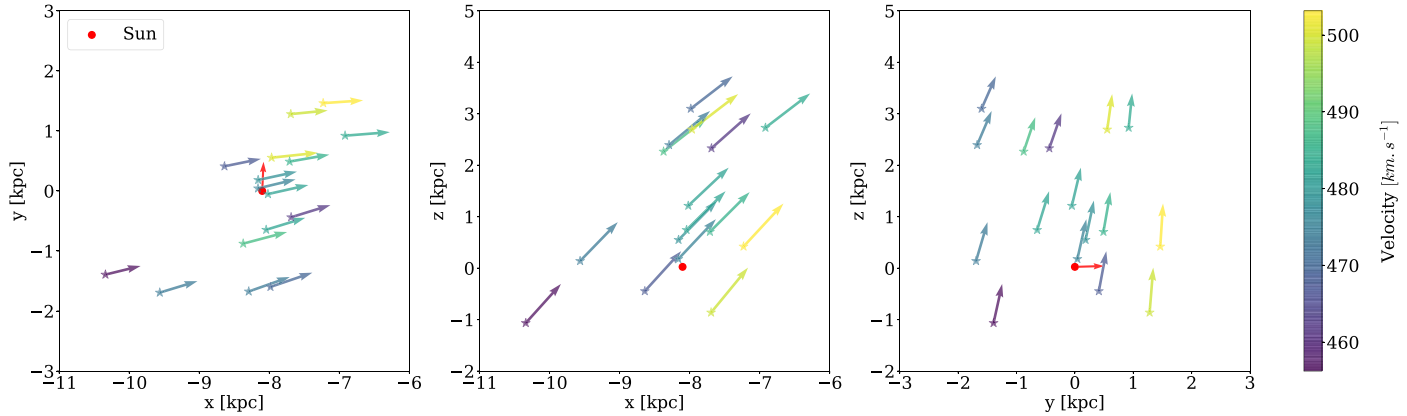

Figure 2. Positions and velocity vectors in galactic Cartesian coordinates of Typhon sample members. Velocity vectors scale 1: 3×10^3. The sample shows very clear streaming motion. For reference, the position and velocity vector of the Sun is also shown in red.

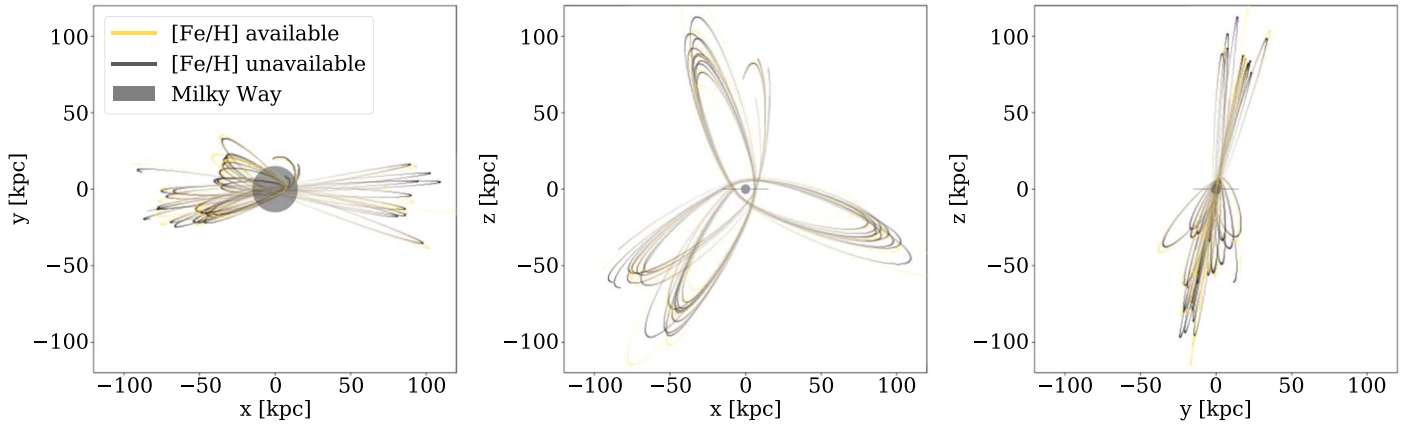

Figure 3. Trajectories of the sample members of Typhon during a 5 Gyr backward integration in the McMillan (2017) potential in Galactic Cartesian coordinates. Trajectories of the seven stars whose metallicity is available through LAMOST DR8 (Wang et al. 2022) are colored in yellow.

as follows: $J_z \in [2000, 3100]$ and $3.3J_\phi + 3500 < J_z < 3.3J_\phi + 5000$, which results in a final sample of 16 stars. This selection box is displayed as a solid black parallelogram in Figure 1.

Furthermore, it should be noted that the symmetric control selection around $J_\phi = 0$, shown as a dashed parallelogram, encompasses only two stars and they do not possess homogeneous dynamical properties. Assuming that the halo is symmetric in angular momentum, there is no a priori reason for the prograde selection to contain significantly more stars than the symmetric retrograde selection as is the case here, other than the selection containing a coherent dynamical group. Taking the symmetric selection as a control sample we estimate the significance of the detection to be $\approx 3.5\sigma$. We note in passing that the Gaia Universe Model Snapshot (GUMS; Robin et al. 2012, updated for Gaia DR3) contains no artificial stars with the selection criteria used to detect Typhon, suggesting that Typhon is a coherent structure that can only be explained by an external body not included in that simulation.

3. Characteristics

The positions and velocities of the sample members of the Typhon stream are shown in Figure 2. We find that member stars of this polar stream are spread out all around us, passing through the solar neighborhood with a high vertical velocity, and exiting the disk at an angle of $\sim 50^\circ$ with respect to it.

In Figure 3 we show the result of integrating Typhon members backward in time for 5 Gyr in the McMillan (2017) Milky Way potential model. Although the stars were selected from a small region in the (J_ϕ, J_z) plane (but with no constraint on J_r), and so should therefore possess similar orbits, there was no a priori reason for the sample to be in phase, as is clearly the case from an inspection of Figure 3. The sample is dynamically coherent, with very similar orbital parameters: $r_{\rm peri} = 6.0 \pm 0.5$ kpc, $r_{\rm apo} = 99 \pm 15$ kpc, $J_r = 6400 \pm 1000$ kpc km s^{-1}, $J_\phi = -560 \pm 110$ kpc km s^{-1}, $J_z = 2500 \pm 300$ kpc km s^{-1}, and eccentricity $e = 0.88 \pm 0.02$.

We estimate the three-dimensional velocity dispersion of the stream to be $\sigma_{v,3D} \approx 13$ km s^{-1} by considering the velocity differences of the stars to the computed orbit of the star with Gaia ID 3939346894405032576 (whose orbit through the solar neighborhood appears closest to the middle of the sample). Assuming isotropy, the one-dimensional velocity dispersion is then $\sigma_v \approx 7.5$ km s^{-1}.

We crossmatched our sample with the LAMOST DR8 (Wang et al. 2022) catalog, in particular the "FEH_PASTEL" column that covers a wide range of metallicities especially on the very metal-poor regime, enabling us to obtain high-quality spectroscopic metallicities for seven stars of the Typhon stream (the stellar parameters of which lie within the reliable range of the PASTEL catalog). These measurements span between [Fe/H] $= -2.23 \pm 0.06$ dex and [Fe/H] $= -1.25 \pm 0.09$ dex.

As shown in Figure 3, where we color orbits of stars of known metallicity in yellow, these stars are dynamically representative of the full sample. In Figure 4 (left panel), we show the likelihood

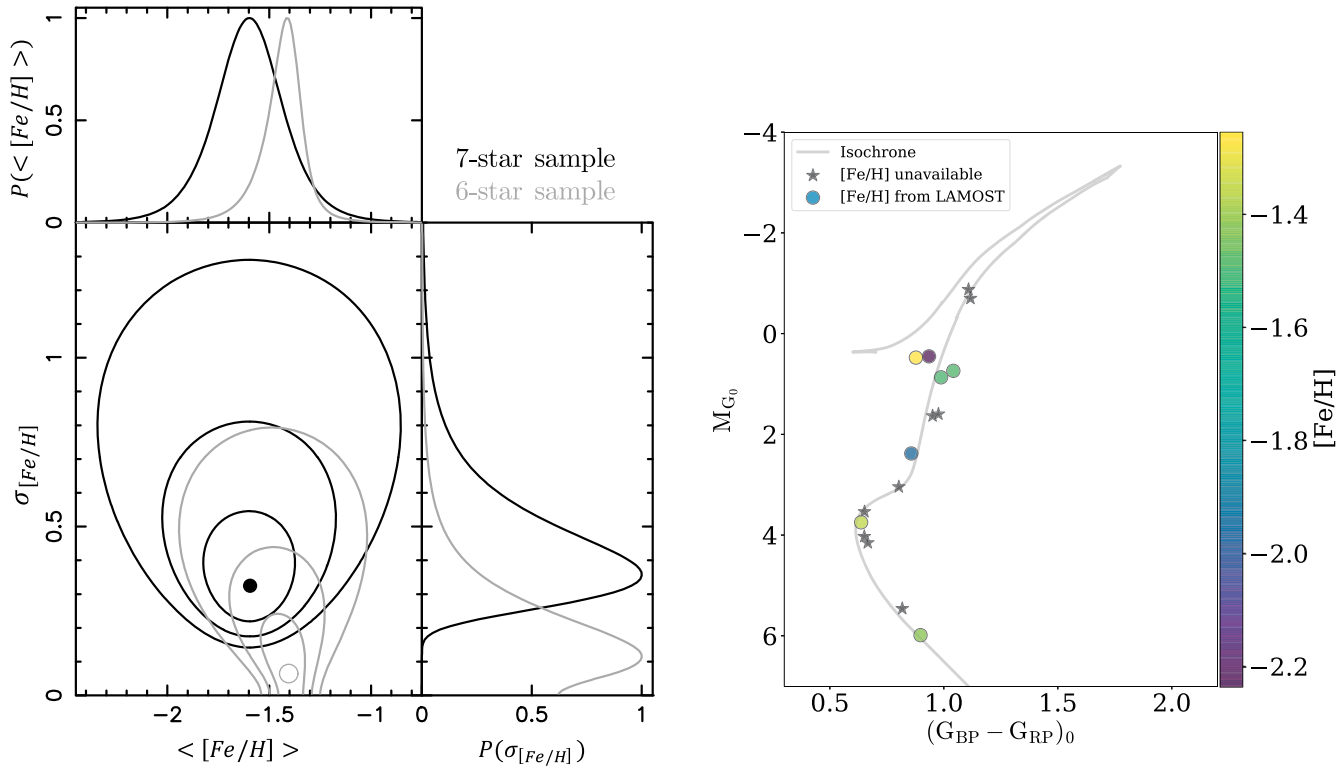

Figure 4. Left: likelihood contours of the mean metallicity and metallicity dispersion of the spectroscopic sample, shown for the full seven-star sample (black lines), and removing the most metal-poor star (gray lines). Right: color–magnitude diagram of the sample members of Typhon. For reference, the gray line shows a PARSEC isochrone model (Bressan et al. 2012) of age 12.5 Gyr and of metallicity [Fe/H] = −1.60 dex. The reasonable correspondence of this model shows that the population is predominantly very old.

Table 1
The Typhon Sample

Gaia Source ID	R.A. (deg)	Decl. (deg)	J_r (kpc km s^{-1})	J_ϕ (kpc km s^{-1})	J_z (kpc km s^{-1})	$r_{\rm peri}$ (kpc)	$r_{\rm apo}$ (kpc)	FeH (dex)
2919273508566727 68	23.65	24.43	5467.78	2109.67	−678.85	5.64	85.13	⋯
1255095276181144320	218.71	25.17	5500.85	2153.71	−641.67	5.65	85.59	-1.42 ± 0.11
1264504793612855808	226.50	24.27	5880.03	2536.48	−561.03	6.11	92.86	-1.50 ± 0.41
1303595799235740288	243.67	25.97	5957.51	2210.55	−625.38	5.63	91.92	⋯
1470463353223683840	205.82	33.33	8919.22	2929.18	−555.25	6.65	138.32	-1.94 ± 0.22
1485076859188949760	212.45	37.57	5789.44	2253.55	−641.30	5.81	90.15	⋯
1765600930139450752	327.45	10.81	7675.31	2069.85	−643.15	5.17	114.35	-2.24 ± 0.06
3013164238138435712	82.50	−10.56	6320.46	2733.22	−343.02	6.15	98.75	⋯
3029220853122930432	115.02	−14.82	6971.03	2793.03	−391.92	6.34	108.47	⋯
3573787693673899520	181.02	−13.37	6106.32	2288.46	−607.18	5.75	94.38	⋯
3736372993468775424	197.96	11.29	4584.30	2469.84	−651.10	6.44	76.04	-1.50 ± 0.09
3793377208170393984	173.49	−2.47	6185.63	2884.76	−441.23	6.65	98.78	-1.25 ± 0.09
3891712266823336192	181.86	1.68	5794.96	3007.81	−400.13	6.87	94.16	⋯
3913243629368310912	178.32	10.63	7589.72	2826.15	−502.54	6.47	118.11	⋯
3939346894405032576	200.01	19.69	6128.64	2412.30	−602.82	5.99	95.58	-1.35 ± 0.07
4537774136693362944	280.74	26.22	7212.08	2163.32	−670.81	5.49	108.86	⋯

Note. Orbital parameters derived using a McMillan (2017) potential. Metallicities from LAMOST DR8 (PASTEL column; Wang et al. 2022) are listed when available.

(This table is available in its entirety in machine-readable form.)

distribution (black contour lines) for the mean metallicity and for the intrinsic dispersion of the metallicity distribution (correcting for the LAMOST uncertainty estimates, assuming that they are reliable). We find $\langle [\mathrm{Fe/H}] \rangle = -1.60^{+0.15}_{-0.16}$ dex and $\sigma([\mathrm{Fe/H}]) = 0.32^{+0.17}_{-0.06}$ dex, which indicates that the system has a resolved dispersion in metallicity. We note, however, that this result depends on the inclusion of the most metal-poor star in the sample; if it is removed (although we have no a priori reason to do so) these values become $\langle [\mathrm{Fe/H}] \rangle = -1.41^{+0.05}_{-0.09}$ dex and $\sigma([\mathrm{Fe/H}]) = 0.06^{+0.17}_{-0.06}$ dex, consistent with no dispersion at the 1σ level.

These metallicities are consistent with the color–magnitude diagram shown in Figure 4, where we use the 3D extinction estimates by Anders et al. (2022) to deredden the stars. In

addition, based on the PARSEC stellar population models (Bressan et al. 2012), and using the canonical two-part power-law initial mass function corrected for unresolved binaries (Kroupa 2001), and Gaia's detection limit, we compute the order of magnitude of the density of the Typhon stream to be of $\sim 25\ M_\odot\,\mathrm{kpc}^{-3}$ in the $d_\odot < 1.5$ kpc solar vicinity fragment. However, without further information we refrain from extrapolating this value out to compute the mass of the full stream structure.

4. Discussion and Conclusions

Although the search for new stellar streams is currently a very active field, to the best of our knowledge the structure discussed here (Typhon) that we isolated thanks to the new and excellent Gaia DR3 data was never identified before. It should be noted that although Typhon is very close to the DTG-11 stream identified in Yuan et al. (2020) in the (J_ϕ, J_z) plane, we verified that Typhon is a distinct structure. In particular, we see that Typhon members have much higher apocenters ($\approx$100 kpc versus $\approx$15 kpc for DTG-11), which becomes obvious when comparing their very different J_r values. In addition, we compared our sample to the thorough Malhan et al. (2022) atlas of stellar streams and found no previously mapped equivalent structure. We note that the discovery of the Typhon structure was confirmed by Dodd et al. (2022) shortly after the first submission of our Letter using a formal clustering metric.

In addition, a follow-up study focusing on the chemical abundances of Typhon was published by Ji et al. (2022). That contribution presents high-resolution spectra for seven Typhon members chosen solely based on observability, including three members whose metallicities are not available in LAMOST DR8, which nevertheless show consistent metallicities with the LAMOST subsample, thereby supporting our conclusions regarding the metallicity distribution of the structure.

The characteristics of Typhon members given in Section 3 lead us to believe that Typhon is likely the tidal remnant of a dwarf galaxy. In particular, the metallicity spread, vertical action spread, and structure width appear completely incompatible with a globular cluster progenitor. With metallicities reaching $[\mathrm{Fe/H}] \sim -1.3$ dex, and with a mean of $[\mathrm{Fe/H}] \sim -1.6$ dex, the mass–metallicity relation of dwarf galaxies (Kirby et al. 2013) suggests that the progenitor likely possessed a luminosity of 10^6–$10^7\ L_\odot$, perhaps similar to the Sculptor dSph. Ji et al. (2022) concur with us on this point. The estimated velocity dispersion value of $\sigma_v \approx 7.5\,\mathrm{km\,s^{-1}}$ lies between that of the Orphan Stream ($\sigma_v \approx 5\,\mathrm{km\,s^{-1}}$; Koposov et al. 2019) and the stream of the Sagittarius dwarf galaxy ($\sigma_v \approx 13\,\mathrm{km\,s^{-1}}$; Gibbons et al. 2017), suggesting that the mass of the Typhon progenitor likely exceeded $10^8 M_\odot$ (an estimate for the mass of Orphan Stream progenitor; Fardal et al. 2019), but was not as massive as the Sagittarius dwarf.

We noticed that although in the heavy McMillan (2017) gravitational potential ($M_{\mathrm{vir}} = 1.3 \times 10^{12} M_\odot$) all stars in the sample are bound, in the lighter MWPotential2014 (Bovy 2015; $M_{\mathrm{vir}} = 8 \times 10^{11} M_\odot$), half of the Typhon stream members are unbound.[5] This underlines how having constraints on the trajectories of streams such as Typhon is of great value as the trajectories of these streams are very dependent on the acceleration field of the Milky Way and its underlying dark matter distribution.

We also checked whether the Typhon members could have close encounters with the Large Magellanic Cloud (LMC) or the Sagittarius dwarf galaxy. Taking the trajectories of the two satellites from Vasiliev et al. (2021), we find that the LMC remains always very distant ($\gtrsim$40 kpc). However, the Typhon stars probably did experience a relatively close flyby of Sagittarius ($\sim$20 kpc, 0.10 Gyr ago). We note that Typhon and Sagittarius share very similar orbital planes, although they possess opposite angular momentum vectors (i.e., the direction of motion in the plane is opposite). The interaction between Typhon and Sagittarius will be interesting to analyze with N-body simulations, but we defer that investigation to a future contribution.

The identification of this high apocenter polar stream passing so close to the Sun raises many questions. Assuming that the solar vicinity is not special and is representative of an average location in the disk, the present detection could be used to place constraints on the number of highly radial accretions that took place during the formation of the Milky Way. The picture suggested by Typhon is that there may be a large population of outer halo dwarf galaxies or dwarf galaxy fragments residing near their apocenters, akin to the "Oort Cloud" around the Sun. A more thorough survey of local phase space for other Typhon-like structures and also deeper next-generation sky surveys (with LSST, for instance) that might detect them in place in the outer halo will help quantify this possibility.

This discovery also underlines the relevance of stream research in the solar vicinity where great quantities of high-quality data are available in addition to spatially wider searches. This poses several challenges and may require the development of new algorithmic approaches suited to exploit Gaia era data for nearby structures with incomplete astrometry (e.g., missing line-of-sight velocities) as sections of streams passing near us are not easily identifiable as streams when projected onto a sky map.

In future work, it will be very useful to attempt to extend the detections along the stream so as to chart it out farther in its orbit through the galaxy. As we alluded to above, such stars may provide very useful dynamical probes for the Milky Way's dark halo, and they will be invaluable to inform follow-up simulation studies attempting to model the N-body evolution of the system. Similarly, having full metallicity information for the member stars would be of great value in order to confirm the present hypothesis regarding the nature of the progenitor.

The authors thank the anonymous referee for their very helpful comments and acknowledge funding from the European Research Council (ERC) under the European Unions Horizon 2020 research and innovation program (grant agreement No. 834148) and from the Agence Nationale de la Recherche (ANR projects ANR-18-CE31-0006, ANR-18-CE31-0017 and ANR-19-CE31-0017). This work has made use of data from the European Space Agency (ESA) mission Gaia (https://www.cosmos.esa.int/gaia), processed by the Gaia Data Processing and Analysis Consortium (DPAC, https://www.cosmos.esa.int/web/gaia/dpac/consortium). Funding for the DPAC has been provided by national institutions, in particular the institutions participating in the Gaia Multilateral Agreement.

[5] Note that none of the Typhon stars were flagged as hypervelocity stars in the Marchetti et al. (2019) census.

Data Availability

The final sample is provided in Table 1 with a more complete table available at doi:10.5281/zenodo.6979887.

ORCID iDs

Wassim Tenachi https://orcid.org/0000-0001-8392-3836
Rodrigo Ibata https://orcid.org/0000-0002-3292-9709
Benoit Famaey https://orcid.org/0000-0003-3180-9825
Zhen Yuan https://orcid.org/0000-0002-8129-5415
Anke Arentsen https://orcid.org/0000-0002-0544-2217
Nicolas Martin https://orcid.org/0000-0002-1349-202X
Akshara Viswanathan https://orcid.org/0000-0002-7507-5985

References

Anders, F., Khalatyan, A., Queiroz, A. B. A., et al. 2022, A&A, 658, A91
Belokurov, V., Zucker, D. B., Evans, N. W., et al. 2006, ApJL, 642, L137
Binney, J., & Tremaine, S. 2011, Galactic Dynamics, Vol. 13 (Princeton, NJ: Princeton Univ. Press)
Bovy, J. 2020, arXiv:2012.02169
Bovy, J. 2015, ApJS, 216, 29
Bressan, Alessandro, Marigo, Paola, Girardi, Léo, et al. 2012, MNRAS, 427, 127
Dodd, E., Callingham, T. M., Helmi, A., et al. 2022, arXiv:2206.11248
Fardal, M. A., van der Marel, R. P., Sohn, S. T., & del Pino Molina, A. 2019, MNRAS, 486, 936
Gaia Collaboration, Vallenari, A., Brown, A. G. A., et al. 2022, A&A, in press
Gaia Collaboration, Prusti, T., de Bruijne, J. H. J., et al. 2016, A&A, 595, A1
Gaia Collaboration, Brown, A. G. A., Vallenari, A., et al. 2021, A&A, 649, A1
Gibbons, S. L. J., Belokurov, V., & Evans, N. W. 2017, MNRAS, 464, 794
Helmi, A. 2008, A&ARv, 15, 145
Helmi, A., White, S. D. M., de Zeeuw, P. T., & Zhao, H. 1999, Natur, 402, 53
Helmi, A., White, S. D. M., & Springel, V. 2003, MNRAS, 339, 834
Ibata, R., Diakogiannis, F. I., Famaey, B., & Monari, G. 2021a, ApJ, 915, 5
Ibata, R., Malhan, K., Martin, N., et al. 2021b, ApJ, 914, 123
Illingworth, J., & Kittler, J. 1988, CVGIP, 44, 87
Ji, A. P., Naidu, R. P., Brauer, K., Ting, Y.-S., & Simon, J. D. 2022, arXiv:2207.04016
Kirby, E. N., Cohen, J. G., Guhathakurta, P., et al. 2013, ApJ, 779, 102
Koposov, S. E., Rix, H.-W., & Hogg, D. W. 2010, ApJ, 712, 260
Koposov, S. E., Belokurov, V., Li, T. S., et al. 2019, MNRAS, 485, 4726
Kroupa, P. 2001, MNRAS, 322, 231
Malhan, Khyati, & Ibata, Rodrigo A 2019, MNRAS, 486, 2995
Malhan, K., Ibata, R. A., Sharma, S., et al. 2022, ApJ, 926, 107
Marchetti, T., Rossi, E. M., & Brown, A. G. A. 2019, MNRAS, 490, 157
McMillan, P. J. 2017, MNRAS, 465, 76
Recio-Blanco, A., de Laverny, P., Palicio, P. A., et al. 2022, arXiv:2206.05541
Robin, A. C., Luri, X., Reylé, C., et al. 2012, A&A, 543, A100
Sanders, Jason L., & Binney, James 2013, MNRAS, 433, 1826
Schonrich, Ralph, Binney, James, & Dehnen, Walter 2010, MNRAS, 403, 1829
Shipp, N., Drlica-Wagner, A., Balbinot, E., et al. 2018, ApJ, 862, 114
Vasiliev, Eugene 2019, MNRAS, 482, 1525
Vasiliev, Eugene, Belokurov, Vasily, & Erkal, Denis 2021, MNRAS, 501, 2279
Wang, C., Huang, Y., Yuan, H., et al. 2022, ApJS, 259, 51
Widmark, A., de Salas, P. F., & Monari, G. 2021, A&A, 646, A67
Yuan, Z., Myeong, G. C., Beers, T. C., et al. 2020, ApJ, 891, 39